



Parametric Study of UC-PBG Structure in Terms of Simultaneous AMC and EBG Properties and its Applications in Proximity-coupled Fractal Patch Antenna

M. M. Fakharian*, P. Rezaei

Department of Electrical and Computer Engineering, Semnan University, Semnan, Iran

PAPER INFO

Paper history:

Received 15 March 2012

Received in revised form 12 June 2012

Accepted 14 June 2012

Keywords:

Uniplanar Photonic Band Gap (UC-PBG)

Artificial Magnetic Conductor (AMC)

Electromagnetic Band Gap (EBG)

Proximity-coupled Fractal Patch Antenna

ABSTRACT

In this paper, a parametric study of conventional Uniplanar Compact Photonic Band Gap (UC-PBG) structures, with different dimensions, is investigated. The studied structure operates as an Artificial Magnetic Conductor (AMC) and Electromagnetic Band Gap (EBG) in which the performances are mainly characterized by the resonant frequency and bandwidth of band gap. Simulation and numerical analysis have been carried out using CST Microwave Studio software, which is based on Finite Difference Time Domain (FDTD), and Ansoft HFSS which is based on Finite Element Method (FEM). Results show that different dimensions affect the AMC's and EBG's performances. The increase in the length and width of the UC-PBG slot will result in lower resonant frequencies and bandwidth degradation, while the frequency band position will increase and the bandwidth of band gap will decrease when the branch width are increased. Furthermore, a prototype of a microstrip line proximity-fed to a fractal patch antenna on a UC-PBG substrate is designed and simulated. Computed results show that the antenna mounted on the UC-PBG substrate has over 9.2% wider impedance bandwidth than the same antenna etched on a grounded dielectric slab with the same characteristics, due to in-phase reflection phase of UC-PBG structure. Compared with the reference antenna at 7.2GHz, the back lobe is reduced by 7.86dB in E plane and 7.68dB in H plane. Cross-polarization level remains below -10dB in both E and H planes.

doi: 10.5829/idosi.ije.2012.25.04a.06

1. INTRODUCTION

Photonic Band-Gap (PBG) or Electromagnetic Band-Gap (EBG) structures are emanated from classical concepts of optics [1]. In recent years, the various applications of these structures have been extended to antenna structures and microwave circuits [2-13]. Practical applications of early EBG designs have some difficulties in accommodating their physical sizes, since the period of an EBG lattice has to be about the half-wavelength at the stop-band. So many small and compact EBG structures have been represented to solve this problem, such as mushroom-like EBG [14], UC-PBG [15], fork-like EBG [16] and spiral-like EBG [17]. In this paper, we focus on Uniplanar Compact PBG (UC-PBG) structures which are realized with square metallic pads connected by narrow strips. Because the whole cells of UC-PBG are on one plane, via holes or multilayer substrates are not required in this structure.

So simplifying the implementation and reducing the costs, the UC-PBG attracts more and more interests.

In a certain frequency range, UC-PBG structures can behave as an EBG surface [15] or as an Artificial Magnetic Conductors (AMC) [18-20], which has made UC-PBG structure very popular in the microwave and antenna research communities. AMCs reflect electromagnetic waves at a frequency called "AMC point" with a zero phase shift (reflection coefficient of +1, in-phase reflection). On the other hand, EBGs do not support surface waves in a frequency interval called the "band gap". In many cases, the AMC point is required to be within the band gap region. Unfortunately, the design of such a structure is rather difficult.

AMC surfaces have found numerous applications as ground planes in printed antennas [21], low profile cavity antennas [18] and as reflectors for aperture coupled patch antennas [22]. AMCs are typically realized based on periodic dielectric substrates and various metallization patterns [23]. In this paper, we specifically study the performance of the conventional

*Corresponding Author Email: m_fakharian@sun.semnan.ac.ir (M. M. Fakharian)

UC-PBG structure operating as AMC and EBG properties in terms of simultaneous by FEM (*HFSS 13*, Ansoft) and FDTD methods (*CST Microwave Studio 2010*) under different dimensions of metallic pad and inductive branch. The effect of various dimensions on the band gap characteristics is out of the scope of this paper and will be the subject of a future research. In particular, study on the effect of the parameters on both the EBG and AMC frequency bands allow the flexibility to design UC-PBG arrays with either one or both of these properties, depending on the requirements of the application. Eventually, this knowledge is employed to design a proximity-coupled fractal patch antenna on the UC-PBG substrate. Simulated results of the realized prototype working at 7GHz show that both wider bandwidth and improvement of radiation pattern can be obtained, in comparison with the same antenna on a conventional substrate.

2. SIMULTANEOUS AMC AND EBG CHARACTERISTICS OF UC-PBG STRUCTURES

Figure 1(a) shows schematic diagrams of the UC-PBG structure, which was designed on a substrate with a thickness of 2mm, relative permittivity of 2.5 (Alone AD 250) and loss tangent 0.003. Each cell of this PBG lattice consists of a square metal pad with four connecting branches, as shown in Figure 1(b). These narrow branches, together with insets at connections, introduce additional inductance seen by the microstrip, and the gaps between neighbor pads enlarge the capacitance [15]. Figure 1(c) shows the equivalent circuit.

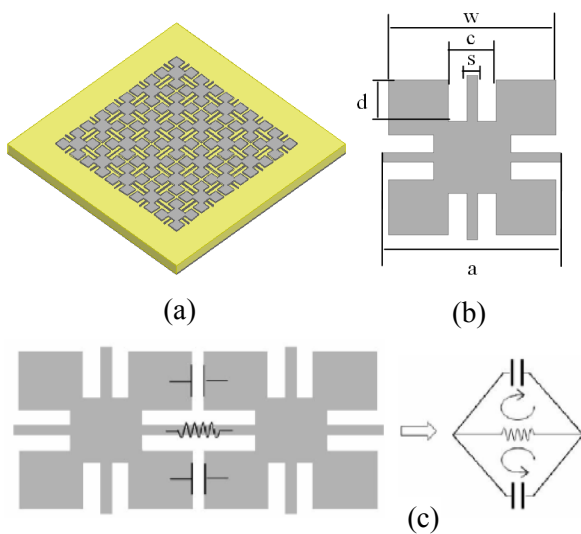


Figure 1. (a) Geometry of the UC-PBG structure. (b) Unit cell of the UC-PBG lattice. (c) The equivalent-circuit.

2. 1. Reflection Phase (AMC) The reflection properties of an AMC structure can be obtained by computing its reflection diagram, which is the graphical representation of the frequency dependence of the phase shift between the incident and reflected wave.

FEM method, based on the Bloch-Floquet theory is used to analyze the reflection phase of UC-PBG structure, and to verify the computation results, the FDTD method is also used for the AMC analysis. A normally incident plane wave is radiated from a source plane, and the reflected fields are calculated at an observation plane, as shown in Figure 2(a). It can be called in-phase (or out-of-phase) reflection, if the reflection phase is 0° (or not). The reflection phase of an AMC surface varies continuously from $+180^\circ$ to -180° relative to the frequency, and crosses zero at just one frequency (for one resonant mode). The useful bandwidth of an AMC is generally defined as $+90^\circ$ to -90° on either side of the central frequency. Periodic Boundary Conditions (PBC) are put on four sides of the unit cell to model the effect of periodic replication in an infinite array structure.

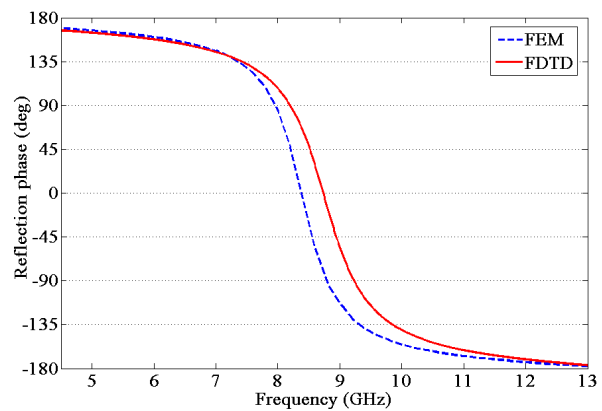
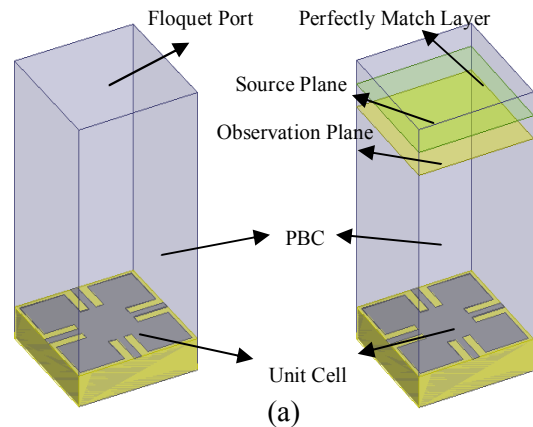


Figure 2. (a) FEM and FDTD simulations model of a UC-PBG unit cell. (b) Results of reflection phase for the UC-PBG structure.

The reflection phase of the reference PBG cell with these parameters is shown in Figure 2(b): the square metal pad size is $w=8\text{mm}$; the inductive branch width is $s=0.5\text{mm}$; the period of cells is $a=8.5\text{mm}$; the width of the slot in metal pad is $c=1.65\text{mm}$ and its length is $d=2.15\text{mm}$. These parameters are seen clearly from Figure 2(b). Although the FEM and FDTD results have a obvious frequency shift, they exhibit the same reflection phase pattern. The resonant frequency is 8.35GHz based on the FEM simulation and 8.71GHz from the FDTD simulation.

2. 2. Dispersion Diagram (EBG) An EBG structure with a forbidden frequency band (no electromagnetic wave propagation is possible), can be fully characterized by its dispersion diagram. The dispersion diagram is a graphical representation of the wave vector in dependence on frequency and gives us information about the position of pass-bands and stop-bands in the frequency spectrum. In particular, a two-dimensional dispersion diagram is desired in order to observe the unit-cell's propagation constant for different angles of an incident wave.

The dispersion diagram of the UC-PBG structure is also simulated using FEM and FDTD methods, as shown in Figure 3(a). Two PBCs are introduced together with a unit-cell of UC-PBG structure and an absorber as lead of the integration box. In FDTD model, Z axis boundaries are either E or H walls, in order to obtain TE and TM modes. To generate the two-dimensional dispersion diagram for the unit-cell of UC-PBG, we have to move along the path Γ to X, X to M, and then M to Γ of irreducible Brillouin zone [24].

The dispersion diagram for the unit cell of Figure 3(a) with the mentioned parameters in section 2.1, are plotted in Figure 3(b). In this diagram, the vertical axis is the frequency and the horizontal axis represents the value of the horizontal wave numbers (K_x, K_y) in Brillouin zone. Each point in the dispersion diagram represents a certain surface wave mode. It is observed that no surface waves can exit in the frequency range from 6.5 to 9GHz for FDTD and 6.31 to 8.65GHz for FEM methods. Thus, this frequency region is defined as a surface wave band gap of the UC-PBG structure.

3. PARAMETRIC STUDY OF THE UC-PBG STRUCTURE

The resonance frequency and the bandwidth for the reflection phase and band gap for the dispersion diagram of UC-PBG structures depend on the unit cell geometry, the substrate's relative permittivity and thickness [25-26]. So, it is important to realize that different dimensions of the same structure result in

different values of resonance frequency and bandwidth for AMC and EBG characteristics. Therefore, in this section the effects of inductive branch width (s), width (c) and length (d) of the slot in metal pads are discussed one by one in order to obtain some guidelines to design a proper UC-PBG surface. Since in the previous section FEM and FDTD methods have shown almost the same results, to simplify the analysis, in this section FEM for AMC analysis and FDTD for EBG analysis, are considered.

3. 1. The Effect of Slot Length in Metal Pad

Length of the slot in metal pad plays an important role in determining the frequency band. To study the effect of this parameter, other parameters such as the inductive branch width and length of the slot in metal pad are kept the same as in previous section. The slot length is changed from 1.5mm to 2.8mm .

Figures 4(a) and 5(a) show the reflection phase of plane waves illuminating and dispersion diagram for the UC-PBG structure respectively with different slot lengths. In addition, Figures 4(b) and 5(b) present the resonance frequency and bandwidth versus the slot length for AMC and EBG, respectively. It is observed that when the slot length is increased, position of the frequency band and bandwidth of band gap will decrease for both AMC and EBG.

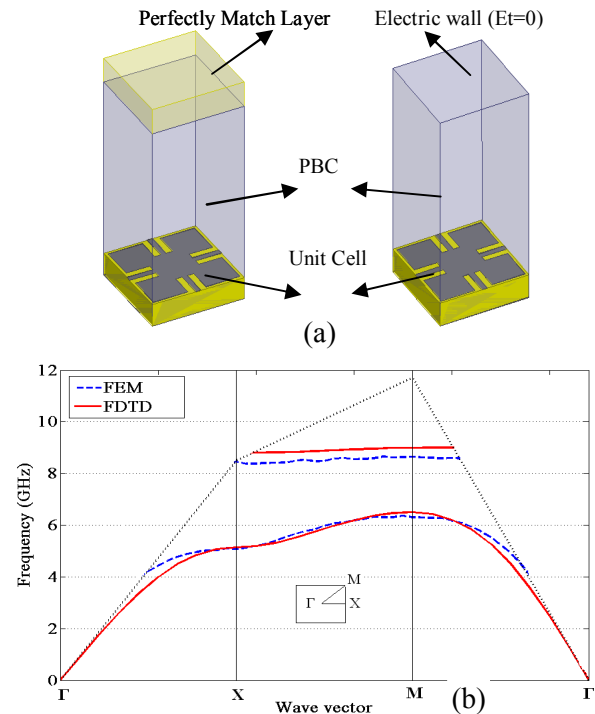


Figure 3. (a) FEM and FDTD simulations model of a UC-PBG unit cell. (b) Results of dispersion diagram for the UC-PBG structure.

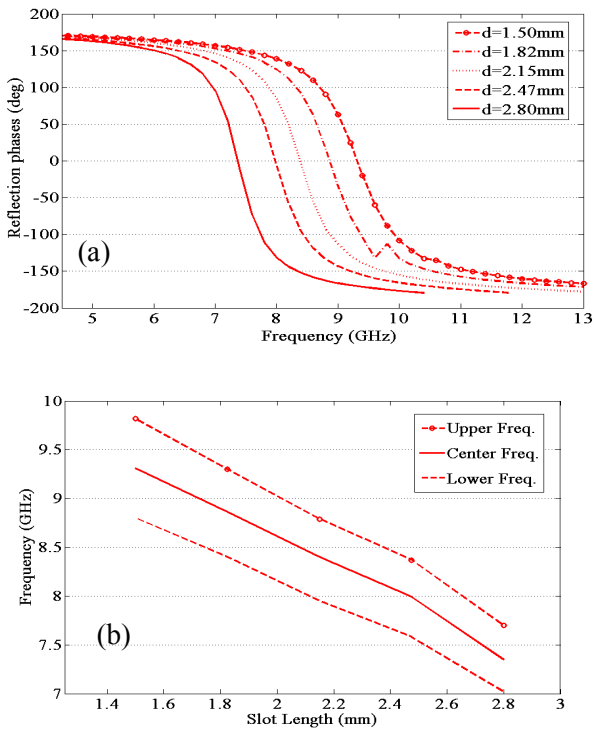


Figure 4. (a) Reflection phase of UC-PBG structure with different slot length. (b) Frequency band and center frequency as functions of the slot length

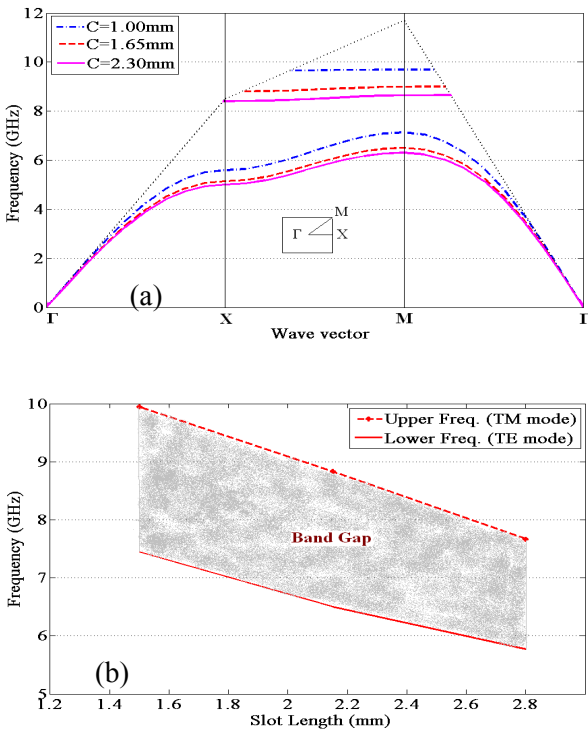


Figure 5. (a) Dispersion diagram of UC-PBG structure with different slot length. (b) Frequency band gap and center frequency as functions of the slot length

3. 2. The Effect of Slot Width in Metal Pad The width of the slot in metal pad determines the distance between inductive branch and metal square pad. Variation of the slot width affects the frequency band of the UC-PBG surface. During this investigation, the slot length and inductive branch width are kept the same as the reference design. The slot width is increased from 1mm to 2.3mm. Figures 6(a) and 7(a) display the reflection phase and dispersion diagram for different slot widths respectively, and Figures 6(b) and 7(b) present the frequency band versus the slot width. It is observed that when the slot width is increased, the resonance frequency will decrease significantly, but the band gap will reduce slightly for both AMC and EBG characteristics.

3. 3. The Effect of Inductive Branch Width Inductive branch width is another effective parameter used to control the frequency band. The UC-PBG structure analyzed in this section has the same parameters as the reference, except the branch width. The branch width is usually kept small; the branch width is increased from 0.25mm to 0.75mm. The reflection phase and band gap positions of dispersion diagram for various branch widths are plotted in Figures 8 and 9. It is observed that the variation of the branch width has the opposite effect on band position to the variation of the slot width and length: as the branch width increases, the frequency band position will increase while the bandwidth for AMC and EBG properties will decrease, as before.

4. PROXIMITY-COUPLED FRACTAL PATCH ANTENNA DESIGN

In this section, a prototype of proximity-coupled fractal patch antenna on a UC-PBG substrate is designed and simulated. Antenna return loss and radiation pattern are investigated and are compared to those of a conventional microstrip patch antenna.

The configuration of a patch antenna with a UC-PBG substrate is depicted in Figure 6. The antenna structure includes three dielectric substrate layers, with parameters $\epsilon_r=2.5$, $h_1=h_2=1\text{mm}$, $h_3=2\text{mm}$ and loss tangent 0.003. The fractal radiation patch is etched above the top substrate, with dimensions of $w=16\text{mm}$, $w_1=4.3\text{mm}$ and $w_2=4.6\text{mm}$ is designed to resonate at 7.2GHz. A 50Ω microstrip line with 1.25mm width is on the middle substrate layer, and is proximity-coupled to the top radiation fractal patch element with inset length of 2mm to the center of the patch. On the lower layer a 5×5 UC-PBG array is placed with the same size as the reference UC-PBG structure in section 2. The CST Microwave Studio and HFSS softwares are used to design the patch antenna.

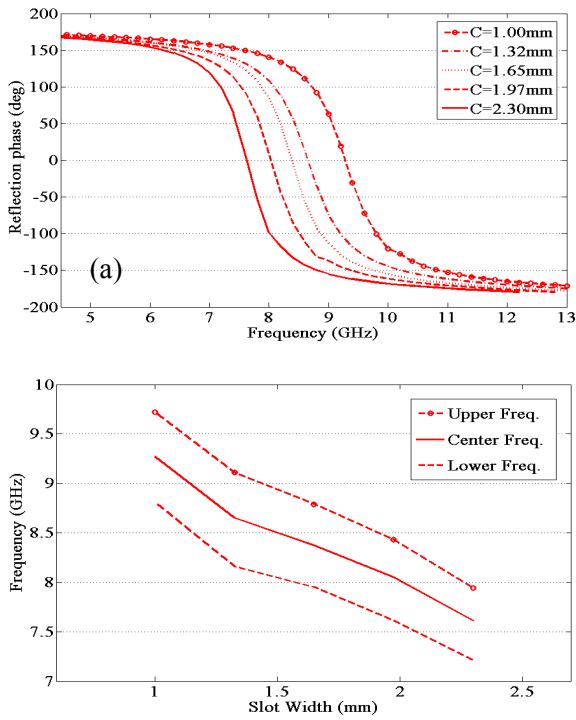


Figure 6. (a) Reflection phase of UC-PBG structure with different slot widths. (b) Frequency band and center frequency as functions of the slot width

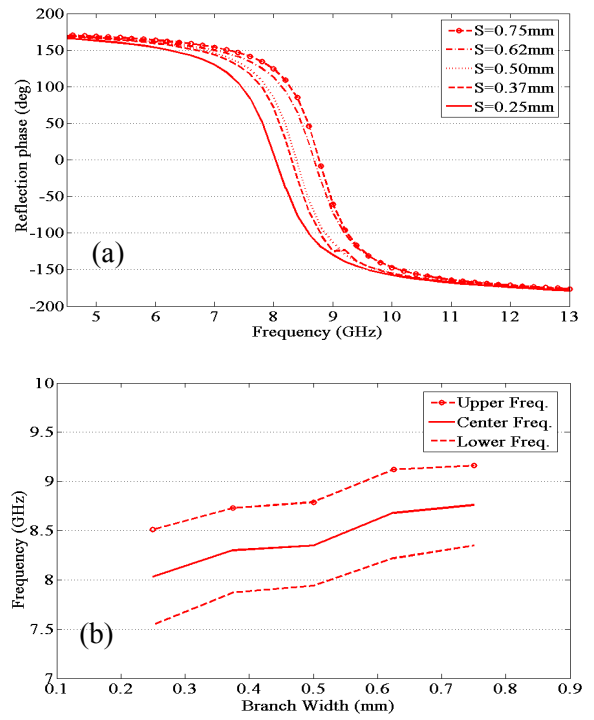


Figure 8. (a) Reflection phase of UC-PBG structure with different branch widths. (b) Frequency band and center frequency as functions of the branch width

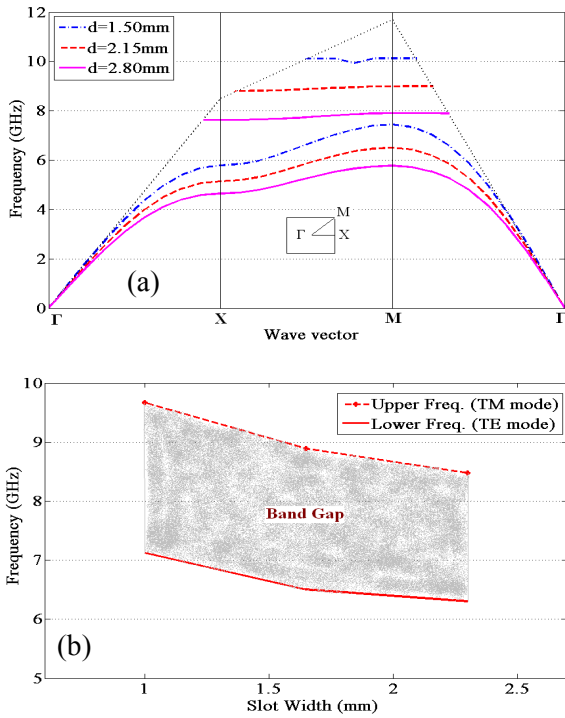


Figure 7. (a) Dispersion diagram of UC-PBG structure with different slot widths. (b) Frequency band gap and center frequency as functions of the slot width

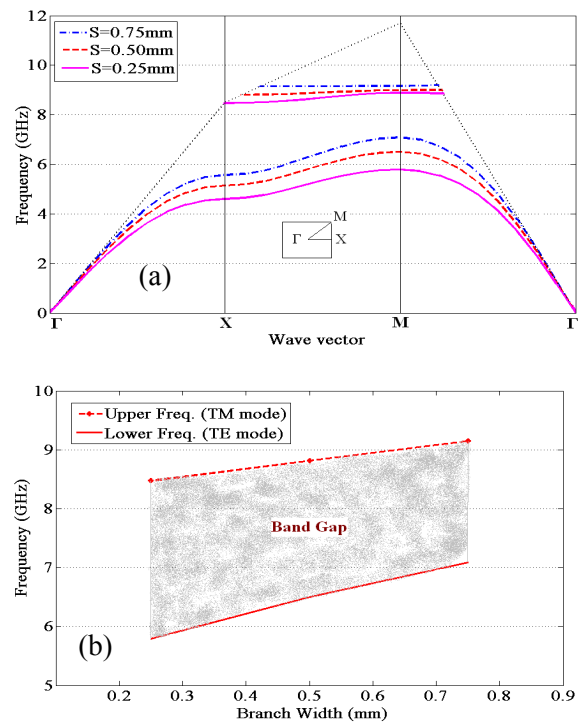


Figure 9. (a) Dispersion diagram of UC-PBG structure with different branch widths. (b) Frequency band gap and center frequency as functions of the branch width

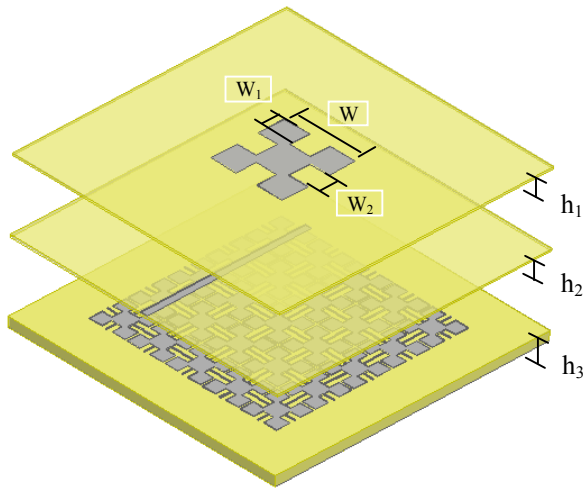


Figure 6. Proximity-fed fractal patch antenna by a microstrip line over a UC-PBG substrate.

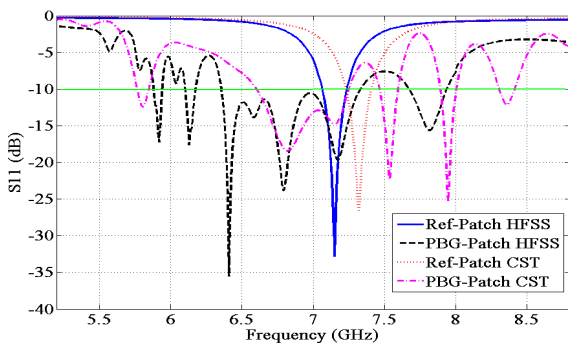


Figure 7. HFSS and CST simulations return loss for the reference and UC-PBG patch antennas.

The simulated results of the return loss (S_{11}) are given in Figure 7. A conventional microstrip antenna with the same size of radiation fractal patch without UC-PBG substrate is also designed and simulated as a reference. The HFSS simulation predicts the resonant frequency at 7.15GHz, while the CST shows the resonance at 7.32GHz, for a normal fractal patch antenna. Its -10dB impedance bandwidth was calculated to be 2.4% for both simulations. In contrast, the resonant frequency of a UC-PBG fractal patch antenna is predicted at 6.79GHz by HFSS simulation, with its -10dB impedance bandwidth of 13% (6.37-7.25GHz) and at 6.9GHz by CST, with its -10dB impedance bandwidth of 10.3% (6.58-7.29GHz), which is about 3% less than the 13% bandwidth computed with HFSS. Both simulation results show that by using UC-PBG patterns in the bottom substrate, the resonant frequency of patch antenna decreases while the impedance bandwidth increases. The discrepancies between HFSS and CST results are basically due to the difference

between their computation methods. The decrease in resonant frequency of a UC-PBG antenna is due to the capacitive and inductive loadings of the PBG profiles under the fractal patch. The increase in bandwidth is due to the fact that the UC-PBG acts like an AMC ground plane for the fractal patch antenna.

The simulated E- and H-plane radiation patterns of the proximity-coupled fractal patch antenna with the UC-PBG substrate of Figure 6, and the reference fractal patch, which differs from that shown in Figure 6 only because it has no UC-PBG, are shown in Figure 8, at 7.2GHz. In both the E-plane (8(a)) and H-planes (8(b)), the patch on the ordinary metal ground plane shows large backward radiations, while the fractal patch antenna on UC-PBG ground plane produces a lower back lobe, with less power wasted in the backward direction. In the H-plane pattern of the fractal patch antenna with PBG, the back lobe is reduced by 5.51dBi in HFSS and 10.21dBi in CST, and in the E-plane pattern, the back lobe is reduced by 5.48dBi with HFSS and 9.89dBi with CST. Furthermore, the boresight gain in CST simulation is 8.41dBi, which is higher than that of the reference patch (7.01dBi). However, it is observed in Figure 8(c), that the component of H-Plane cross-polarization radiation is increased by using UC-PBG substrate. The H-plane cross-polarization has a peak level of -10.3dBi, which is higher than that of the reference antenna (-18.1dBi) in CST simulation. Whereas the E-plane cross-polarization pattern is negligible being lower than -30dBi, it is not depicted.

5. CONCLUSION

The performances of the conventional UC-PBG structure operating as an AMC and EBG were investigated under different dimensions. Our numerical analysis shows that the reflection phase curve and the dispersion diagram which is employed to infer the AMC and EBG characterizes respectively are affected by different dimensions of slot length, slot width and inductive branch width. A shift to a lower AMC resonance frequency and EBG is observed in addition to degradation in the operational bandwidth of band gap when the slot length and width are increased, while the variation in the branch width has the opposite effect on band position. It is concluded that this type of study is important to design AMC and EBG structures for various applications of UC-PBG, where the operating frequency and bandwidth are the cornerstones of the performance. Besides, using the UC-PBG as the substrate of a fractal patch antenna, an impedance bandwidth of 11.65% is obtained, that is significantly higher than that of the reference conventional patch antenna. In addition, the proximity-coupled-fed fractal patch mounted on the UC-PBG plane has shown a great

improvement in radiation performance with respect to the same patch etched on a conventional substrate. Results show an achievement of a more focused beam radiated in the broadside direction with over 1.4dB directive gain improvement at broadside direction, as well as 7.86dB reduction of the back lobe in the H-plane, while maintaining the level of cross polarization below -10dB. Therefore, we can conclude that using a UC-PBG as the substrate of proximity-coupled fractal patch antenna improves its performance, both in bandwidth and radiation pattern.

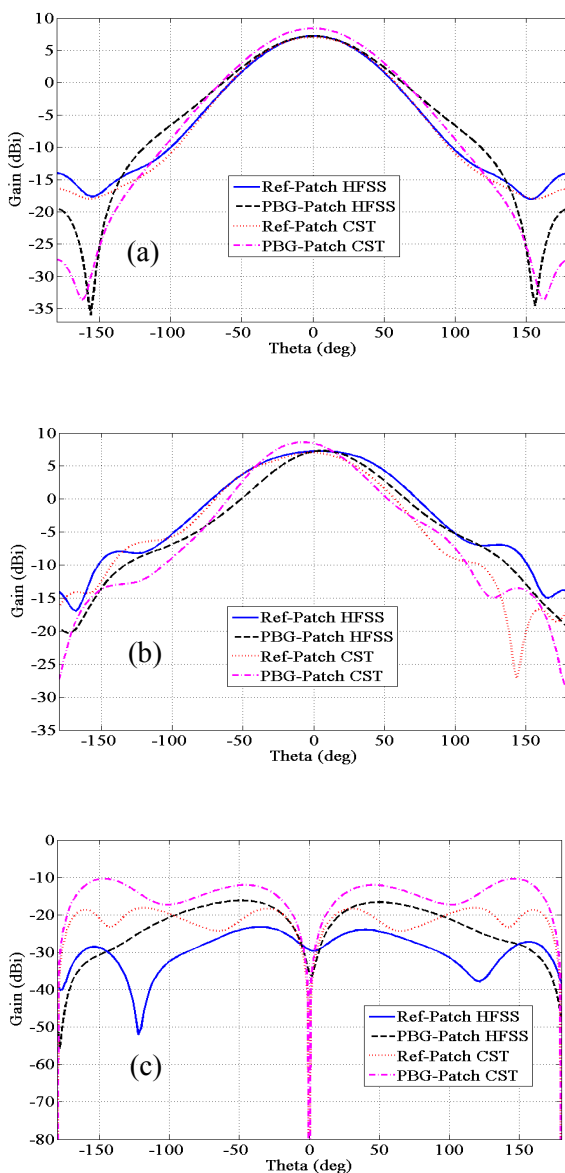


Figure 8. HFSS and CST simulations (a) H-plane, co-polar (b) E-plane, co-polar and (c) H-plane, cross-polar components radiation pattern of reference and UC-PBG antenna, at 7.2GHz.

6. ACKNOWLEDGMENT

The authors would like to acknowledge the assistance and financial support provided by the Office of Brilliant Talents at the Semnan University, and reviewers' valuable comments.

7. REFERENCES

- Joannopoulos, J. D., Johnson, S. G., Winn, J. N. and Meade, R. D., "Photonic Crystals: Molding the Flow of Light," 2nd Edition, *Princeton University Press*, (2008).
- Yang, F. and Rahmat-Samii, Y., "Electromagnetic Band-gap Structures in Antenna Engineering," *Cambridge University Press*, Cambridge, UK, (2008).
- Yang, F. R., Ma, K. P., Qian, Y. and Itoh, T., "A uniplanar compact photonic-bandgap (UC-PBG) structure and its applications for microwave circuit," *IEEE Transaction on Microwave Theory and Techniques*, Vol. 47, No. 8, (1999), 1509-1514.
- Fakharian, M. M. and Rezaei, P., "Design of a New Compact EBG Structure and its Application in Inset Feed Fractal Microstrip Patch Antenna Arrays" *IEEE International RF and Microwave Conference*, (2011), 246-249.
- Yang, F. and Rahmat-Samii, Y., "Microstrip antennas integrated with electromagnetic band-gap (EBG) structures: A low mutual coupling design for array applications," *IEEE Transaction on Antennas and Propagation*, Vol. 51, No. 10, (2003), 2936-2946.
- Qu, D., Shafai, L. and Foroozesh, A., "Improving microstrip patch antenna performance using EBG substrates," *IEEE Proceedings Microwaves, Antennas and Propagation*, Vol. 153, No. 6, (2006), 558-563.
- Fakharian, M. M. and Rezaei, P., "Numerical Analysis of Mushroom-Like and Uniplanar EBG Structures Utilizing Spin Sprayed Ni (-Zn)-Co Ferrite Films For Planar Antenna", *European Journal of Scientific Research*, Vol.73, No.1, (2012), 41-51.
- Shaban, H. F., Elmikaty, H. A. and Shaalan, A. A., "Study the effects of electromagnetic band gap (EBG) substrate on two patches microstrip antenna," *Progress In Electromagnetics Research B*, Vol. 10, (2008), 55-74.
- Chang, C. P., Su, C. C., Hung, S. H., Wang, Y. H. and Chen, J. H., "A 6:1 unequal Wilkinson power divider with EBG CPW," *Progress In Electromagnetics Research Letters*, Vol. 8, (2009), 151-159.
- Kim, Y. J., Yang, K. B. and Kim, Y. S., "Wideband simultaneous switching noise suppression in mobile phones using miniaturized electromagnetic bandgap structures," *Journal of Electromagnetic Waves and Applications*, Vol. 23, No. 14, (2009), 1929-1938.
- He, Y., Li, L., Liang, C. H. and Liu, Q. H., "EBG structures with fractal topologies for ultra-wideband ground bounce noise suppression," *Journal of Electromagnetic Waves and Applications*, Vol. 24, No. 10, (2010), 1365-1374.
- Arghand Lafmajani, I. and Rezaei, P., "A novel frequency-selective metamaterial to improve helix antenna," *Journal of Zhejiang University Science C*, Vol.13, No.5, (2012), 365-375.
- Fakharian, M. M., "Design of Compact Wideband and Multiband Fractal EBG Structure for Microstrip Antenn," *IEEE International RF and Microwave Conference*, (2011), 234-237.
- Sievenpiper, D., Zhang, L., Broas, R. F. J., Alex opoulos, N. G. and Yablonovitch, E., "High-impedance electromagnetic surfaces in a forbidden frequency band," *IEEE Transaction on*

- Microwave Theory and Techniques*, Vol. 47, (1999), 2059-2074.
15. Coccioli, R., Yang, F. R., Ma, K. P. and Itoh, T., "Aperture-coupled patch antenna on UC-PBG substrate," *IEEE Transaction on Microwave Theory and Techniques*, Vol. 47, (1999), 2123-2130.
 16. Li, Y., Fan, M., Chen, F., She, J. and Feng, Z., "A novel compact electromagnetic-bandgap (EBG) structure and its applications for microwave circuits," *IEEE Transaction on Microwave Theory and Techniques*, Vol. 53, (2005), 183-190.
 17. Zheng, Q. R., Lin, B. Q., Fu, Y. Q. and Yuan, N. C., "Characteristics and applications of a novel compact spiral electromagnetic band-gap (EBG) structure," *Journal of Electromagnetic Waves and Applications*, Vol. 21, No. 2, (2007), 199-213.
 18. Feresidis, A. P., Wang, S. and Vardaxoglou, J. C., "Artificial magnetic conductor surfaces and their application to low-profile high-gain planar antennas," *IEEE Transaction on Antennas and Propagation*, Vol. 53, No. 1, (2005), 209-215.
 19. Yang, F. and Rahmat-Samii, Y., "Reflection phase characterizations of the EBG ground plane for low profile wire antenna applications," *IEEE Transaction on Antennas and Propagation*, Vol. 51, No. 10, (2003), 2691-2703.
 20. De Cos, M. E., Alvarez, Y., Hadarig, R. C. and Las-Heras, F., "Novel SHF band uniplanar Artificial Magnetic Conductor," *IEEE Antennas and Wireless Propagation Letters*, Vol. 9, (2010), 44-47.
 21. Mosallaei H. and Sarabandi, K., "Antenna miniaturization and bandwidth enhancement using a reactive impedance substrate," *IEEE Transaction on Antennas and Propagation*, Vol. 52, No. 9, (2004), 2403-2414.
 22. Zhang, Y., von Hagen, J., Younis, M., Fischer, C. and Wiesbeck, W., "Planar Artificial Magnetic Conductors and Patch Antennas," *IEEE Transaction on Antennas and Propagation, Special Issue on Metamaterials*, Vol. 51, No. 10, (2003), 2704-2712.
 23. Barlevy, A. S. and Rahmat-Samii, Y., "Characterization of electromagnetic band-gaps composed of multiple periodic tripods with interconnecting vias: Concept, analysis, and design," *IEEE Transaction on Antennas and Propagation*, Vol. 49, No. 3, (2001), 343-353.
 24. Kittel, C., Introduction to Solid State Physics, 7th Ee. New York: Wiley Text Books, 1964.

Parametric Study of UC-PBG Structure in Terms of Simultaneous AMC and EBG Properties and its Applications in Proximity-coupled Fractal Patch Antenna

M. M. Fakharian, P. Rezaei

Department of Electrical and Computer Engineering, Semnan University, Semnan, Iran

PAPER INFO

چکیده

Paper history:

Received 15 March 2012

Received in revised form 12 June 2012

Accepted 14 June 2012

Keywords:

Uniplanar Photonic Band Gap (UC-PBG)

Artificial Magnetic Conductor (AMC)

Electromagnetic Band Gap (EBG)

Proximity-Coupled Fractal Patch Antenna

در این مقاله، مطالعه پارامتری ساختار فشرده مسطح واحد (Uniplanar)، با ابعاد متفاوت، مورد بررسی قرار گرفته شده است. ساختار مورد مطالعه در عمل به عنوان یک هادی مغناطیسی مصنوعی (AMC) و باندممنوعه الکترومغناطیسی (EBG) در نظر گرفته شده که عملکرد آنها به طور معمول توسط فرکانس تشدید و پهنای باند باندممنوعه مشخص می‌شود. مدلسازی و تحلیل عددی توسط نرم‌افزارهای CST بر اساس روش تفاضل محدود و HFSS بر اساس روش اجزاء محدود انجام شده است. تاثیر ابعاد مختلف بر عملکرد AMC و EBG در نتایج مشخص شده است. افزایش در طول و عرض شکاف UC-PBG منجر به کاهش فرکانس تشدید و تنزل پهنای باند است، در حالی که موقعیت باند فرکانسی افزایش می‌یابد و پهنای باند آنها کاهش خواهد یافت هنگامی که عرض شاخه افزایش داده شود. علاوه بر این، یک نمونه اولیه از یک آنتن پیچ فراکتال با تغذیه مجاورتی بر روی زیرلایه UC-PBG طراحی و شبیه‌سازی شده است. نتایج محاسبه شده نشان می‌دهد که آنتن نصب شده بر روی زیرلایه UC-PBG، با توجه به انعکاس هم‌فاز در فاز ساختار UC-PBG، پهنای باند امیدانسی بیش از ۹/۲٪ وسیع‌تر از همان آنتن بر روی یک لایه دی‌الکتریک معمولی با همان خصوصیات مشابه دارد. در مقایسه با آنتن منفرد در فرکانس ۷/۲ گیگاهرتز، لوب پشتی در صفحه E به میزان ۷/۸۶ دسی‌بل و در صفحه H به ۷/۶۸ دسی‌بل کاهش داشته است. سطح پلاریزاسیون متعامد در صفحات E و H کمتر از ۱۰- دسی‌بل باقی مانده است

doi: 10.5829/idosi.ije.2012.25.04a.06